NEW CARBON MATERIALS
Volume 29, Issue 1, Feb 2014
Online English edition of the Chinese language journal

Available online at www.sciencedirect.com
ScienceDirect

Cite this article as: New Carbon Materials, 2014, 29(1):34–40.

RESEARCH PAPER

Field emission properties of carbon nanocoils synthesized on stainless steel

Li-li Li, Lu-jun Pan*, Da-wei Li, Qin Zhao, He Ma

School of Physics and Optoelectronic Technology, Dalian University of Technology, Dalian 116023, China

Abstract: Carbon nanocoils (CNCs) were synthesized by a thermal chemical vapor deposition (CVD) method over tin-coated type 202 stainless steel (SS) plates (Cr 15%, Mn 10%, Ni 1%). It is considered that the calcination at 900 °C leads to the crazing of the SS surface, which causes the Fe (Ni) and Sn to be fully mixed and forms active Fe (Ni)-Sn-O catalyst particles suitable for the growth of CNCs. However, the Cr in the catalyst particles is below the limitation of detection, and its role is currently not understood. The electron field-emission properties of as-grown CNCs dispersed on an n-type Si substrate were also investigated. It is found that the CNCs exhibit a low turn-on electric field of 1.6 V/m. The distributions of electric fields on a stand-up and a laid-down CNC successfully explain the behavior of the Fowler-Nordheim (*F-N*) plot. The field enhancement factor for the laid-down CNC is 2.25 times larger than that for a laid-down multiwall carbon nanotube (CNT). This is because the helical morphology of the CNCs can reduce the screening effect produced by the surrounding substrate. In this case, CNCs can more easily emit electrons, and show promise for use in X-ray sources, field emission displays and other micro- or nano-devices.

Key Words: Carbon nanocoils; Stainless steel; Calcination temperature; Field emission; Finite element method

1 Introduction

Carbon nanocoils (CNCs) have attracted much attention because of their excellent mechanical and electrical properties [1,2]. They were mostly synthesized by chemical vapor deposition (CVD) method [3,4]. Generally, CNCs were synthesized on Fe-Sn-coated Si/SiO_2 substrates, or Fe-coated indium-tin-oxide glass substrates [5-7] etc. In the mass production of CNCs, it is too expensive to use these substrates. Recently, Chang et al [3] have synthesized CNCs with a high yield on a low price 304 stainless steel plate (Cr 18%, Ni 8%) with Sn spin-coated on it. In this work, Sn-coated ordinary SS plate（Cr 15.27%, Mn 10.11%，Ni 1.32%）, which is cheaper than 304 SS plate, has been used to synthesize high-yield CNCs. The influence of the calcination temperature on the CNC growth was also investigated.

It is known that carbon-based nanomaterials, especially carbon nanotubes (CNTs) have excellent field emission properties, which are expected to be applied in electron guns, field emission displays and other electronic devices [8-11]. So far, there are two main methods to fabricate CNT emitters. One is directly growth of CNT array on patterned electrodes [12]. However, the distribution of electric fields on these CNT arrays are not uniform and strongly concentrated at the edge of the arrays [12,13]. The other is screen-printing method that prints the mixture of CNTs and binders on electrodes [14], but, most of the CNTs are laid down on the substrate when using the screen-printing method. The laid-down CNTs cannot easily emit electrons, and the turn-on voltage is high [15] that largely limit their applications. CNCs, another kind of carbon nanomaterials, also possess excellent field-emission properties owing to their unique spiral morphologies. It is considered that the electrons can be emitted not only from the tip of a CNC, but also from its side body and the outstanding performance is also attributed to the high aspect ratio of the CNCs [16-19]. Therefore, the efficiency of field emission from CNCs is considered to be higher than CNTs and is suitable for wide applications. In this work, we have studied the field-emission properties of the CNCs dispersed on an n-type Si substrate by considering the case of screen-printing. The distributions of electric fields on a stand-up /a laid-down CNC and a laid-down CNT were calculated by a finite element method.

2 Experimental

An ordinary SS plate with a thickness of 360 μm was selected as the substrate. A $SnCl_2{\cdot}2H_2O$ ethanol solution with a concentration of 0.025 mol/l was used as the catalyst precursor and dropped to the SS substrates. Then the samples were calcined at temperatures of 700, 800 and 900 °C in air for 30 min. Finally, the calcined SS samples were put into a CVD chamber to synthesize the CNCs at 700 °C for 60 min under the flow of acetylene and argon with flow rates of 17 and 323 mL/min, respectively. The carbon deposits and the calcined samples were observed and analyzed by a scanning electron microscope. The field-emission properties of

Received date:23 April 2013; **Revised date:** 25 October 2014
***Corresponding author.** E-mail: lpan@dlut.edu.cn
†These authors equally contributed to this work.

DOI: 10.1016/S1872-5805(14)60123-2

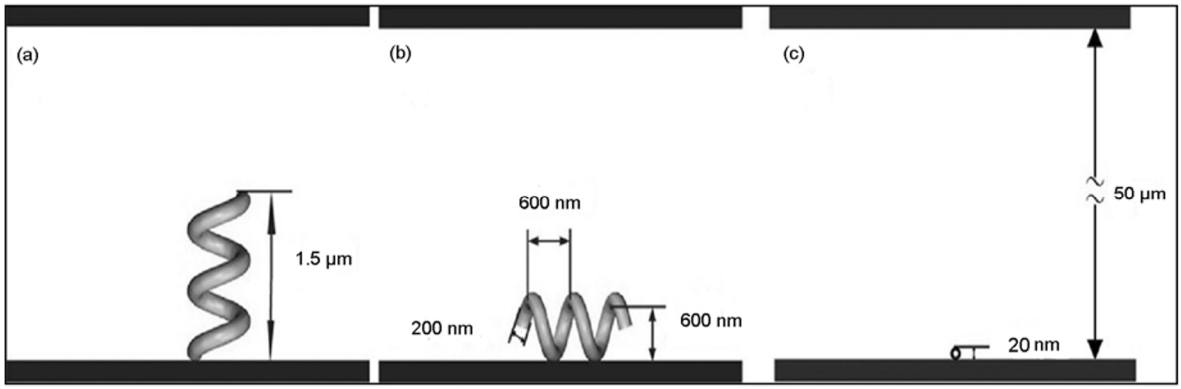

Fig. 1 Simulation models for the field-emission devices using (a) a stand-up CNC, (b) a laid-down CNC and (c) a laid-down CNT as the emitters.

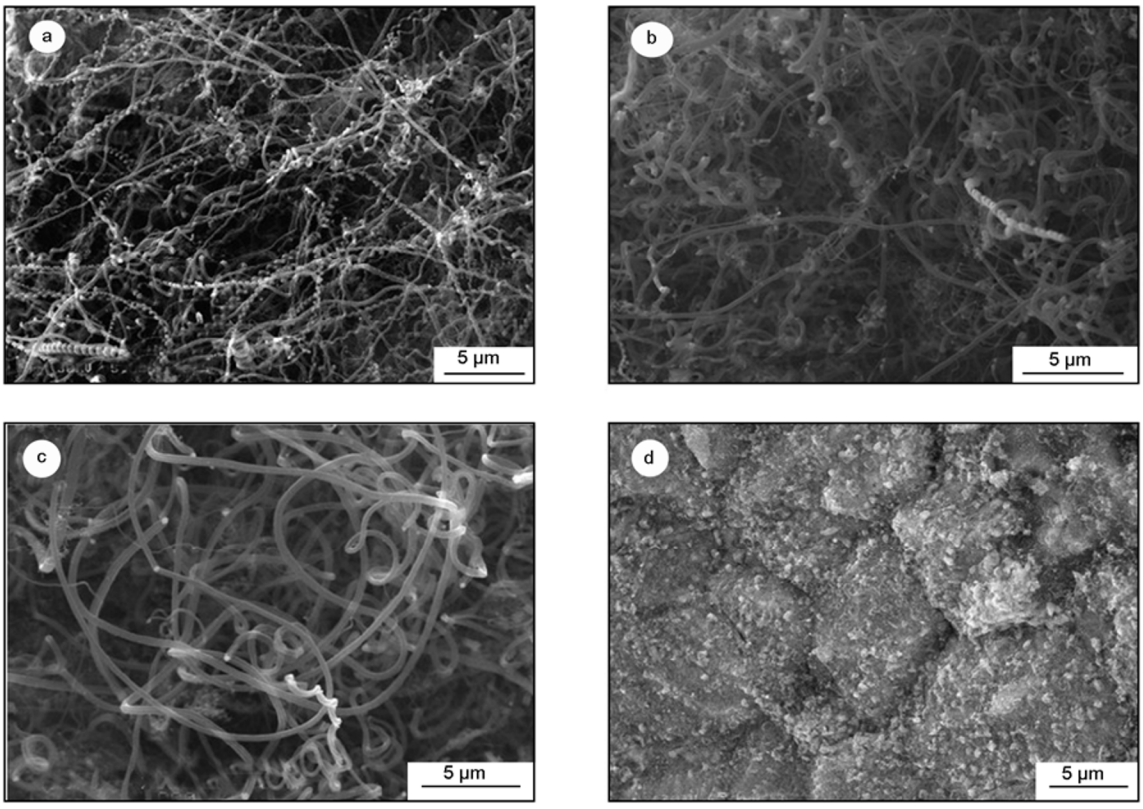

Fig. 2 SEM images of carbon deposits grown on the Sn-coated SS substrates which were initially calcined at (a) 900 °C, (b) 800 °C, (c) 700 °C and (d) 1000 °C.

as-grown CNCs were studied by using a diode-type configuration in a vacuum chamber at a base pressure lower than 4×10^{-5} Torr. An n-type Si substrate with CNCs uniformly dispersed on its surface was used as the cathode and an indium tin oxide (ITO) glass plate as the anode. The gap between the anode and cathode was set to be 350 μm.

In addition, the distributions of electric fields on a stand-up CNC, a laid-down CNC and a laid-down CNT were calculated by a three-dimensional finite element method. The model used is shown in Fig. 1, where the space between the two parallel electrodes was set to be 50 μm, and the applied voltage ranged from 75 to 305 V. Line diameter, coil diameter and pitch of the CNC are 200, 600 and 600 nm, respectively, which correspond to the parameters of the actually grown CNCs, and its length is set to be 1.5 μm. For comparison, the CNT diameter is set to be 20 nm, which is the same as the diameter of CNT synthesized in the general experiment conditions.

3 Results and discussion

Figs. 2a, 2b and 2c show the SEM images of the deposits

grown on the substrates which were initially calcined at 900 °C, 800 °C, and 700 °C, respectively. At the calcination temperature of 900 °C, the deposits are almost CNCs with an average line diameter, coil diameter and pitch of 220, 602 and 601nm, respectively. When the calcination temperature is decreased to 700 °C, there are almost no CNCs but carbon nanofibers (CNFs) are grown, and a mixture of CNCs and CNFs are obtained on the sample initially calcined at 800 °C. An attempt was made to use a higher calcination temperature of 1000 °C to pretreat the Sn-coated SS plate, but the deposits after CVD are mainly some carbon grains, as shown in Fig. 2d. These results show an obvious dependence of the yield of CNCs on the calcination temperature.

Figs. 3a-c show the SEM images of the pure SS substrates after calcination at 700, 800 and 900 °C, respectively. Chang et al. have reported that oxidation is effective for forming cracks on the surface of SS plates [3]. It is observed that with increasing calcination temperature, the cracks on the surface of SS substrate become more serious and can be clearly observed in Fig. 3c, where the SS substrate was calcined at 900 °C. It is considered that this kind of large porous structure and rough surface is beneficial for the sufficient fusion of added Sn with Fe(Ni) in the SS substrate. The corresponding SEM images of Sn-coated SS substrates are shown in Figs. 3d-f. It is found that with increasing calcination temperature, the catalysts are distributed more uniformly and changed from large islands at 700 and 800 °C to isolated small particles at 900 °C. This

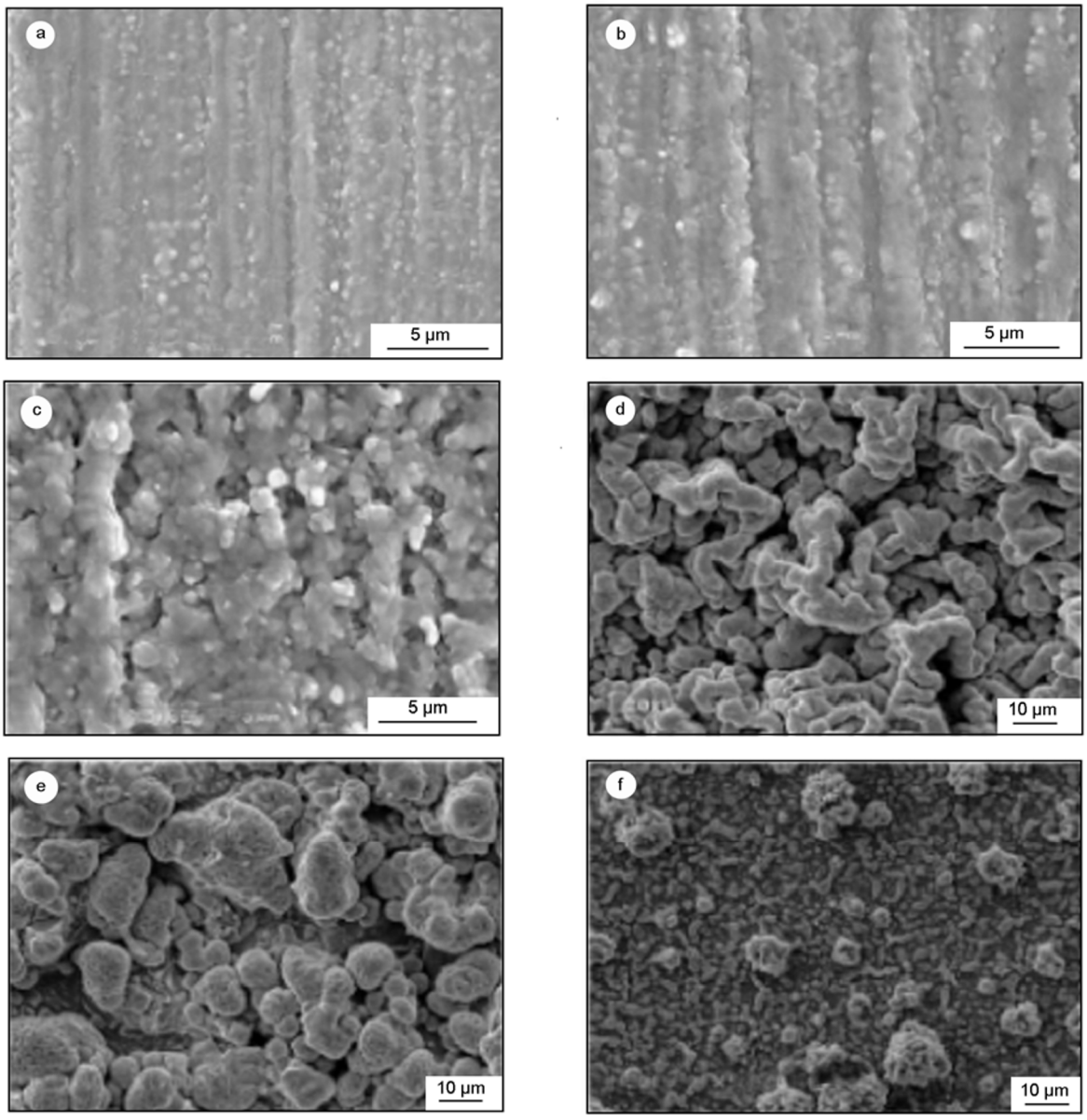

Fig. 3 SEM images of pure SS substrates after calcination at (a) 700 °C, (b) 800 °C and (c) 900 °C, and the corresponding SEM images of Sn-coated SS substrates after calcination at (d) 700 °C, (e) 800 °C and (f) 900 °C.

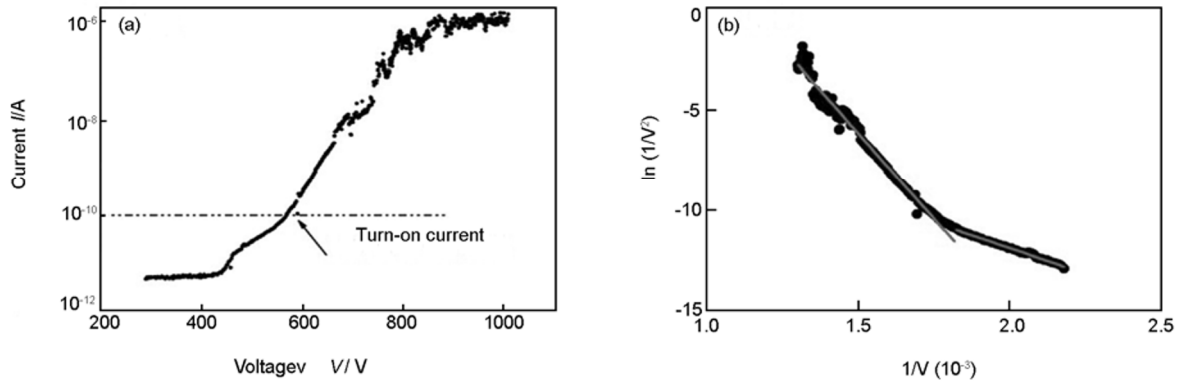

Fig. 4 (a) Curve of emission currents vs. applied voltages for the CNCs dispersed on the n-type Si substrate and (b) the Fowler-Nordheim (*F-N*) plot relevant to (a).

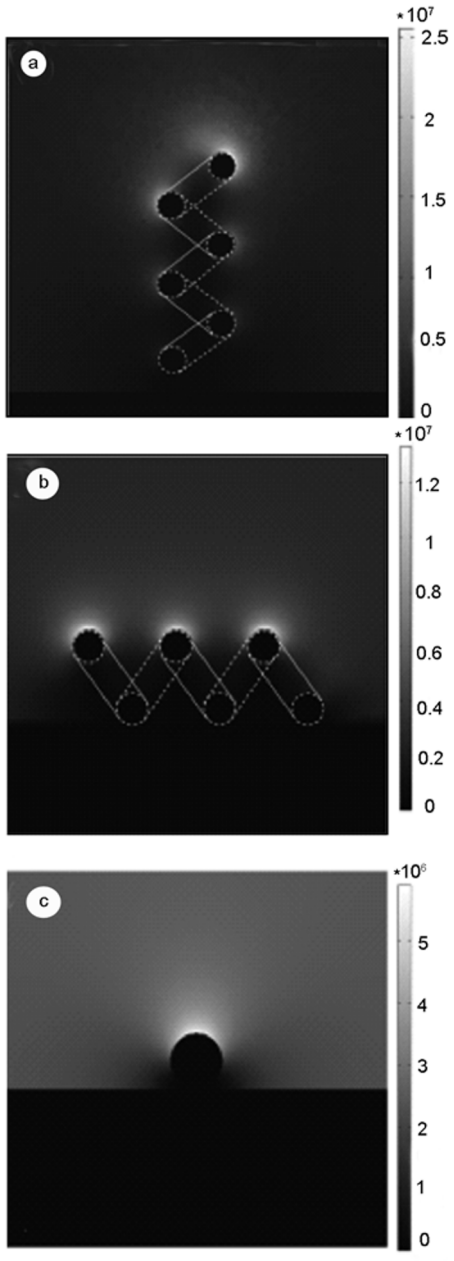

Fig. 5 Electric field strength profiles for a slice around middle cross section of (a) a stand-up CNC, (b) a laid-down CNC and (c) a laid-down CNT under the anode voltage of 105 V.

behavior is resulted from the porous surface structure of the cracked SS substrate. It is considered that the Fe-Sn (Ni)-O catalyst particles with a relatively uniform distribution are formed on the SS surface at the calcination temperature of 900 ^{o}C, which contribute to the growth of CNCs. Therefore, the calcination temperature is crucial in synthesizing CNCs by using SS substrates.

Fig. 4 shows (a) the *I-V* curve of the CNC emitter and (b) the relative *F-N* plot. As shown in Fig. 4a, the turn-on voltage for the CNC emitter, defined as the voltage when the emission current reaches 10^{-10} A, has a relatively low value of 568 V, corresponding to average electric field strength of 1.6 V/μm. This value is comparable to those of the reported stand-up CNT emitters, which is lower than those of the CNT emitters laid down on the substrates [15,16]. As shown in Fig. 4b, the *F-N* plot consists of two straight lines.

According to the *F-N* theory, the field-emission current can be written as [20,21]

$$\ln(\frac{I}{V^2}) = \ln\frac{A\alpha\beta^2}{\varphi} - B\frac{\varphi^{1.5}}{\beta}.\frac{1}{V}$$

where I is the emission current, V is the voltage between the anode and cathode, ϕ is the work function, α is the effective area of field emission, A and B are constants, β is the field enhancement factor. Therefore, the slope of the *F-N* plot is $-B\,\phi^{1.5}/\beta$.

Considering that the value of work function ϕ for CNCs is the same, so the absolute slope value of *F-N* plot is inversely proportional to β. The grown CNCs are dispersed on the n-type Si substrate, with almost the CNCs laid down on the substrate. With the increase of applied voltage, the Coulomb force between the CNCs and anode plate increases, leading to the standing up of some CNCs from their one ends with the other ends still attached on the substrate. It is considered that the stand-up CNCs contribute to the straight line where the values of $1/V$ are less than 1.82 in the *F-N* plot and the laid-down CNCs contribute to the other straight line.

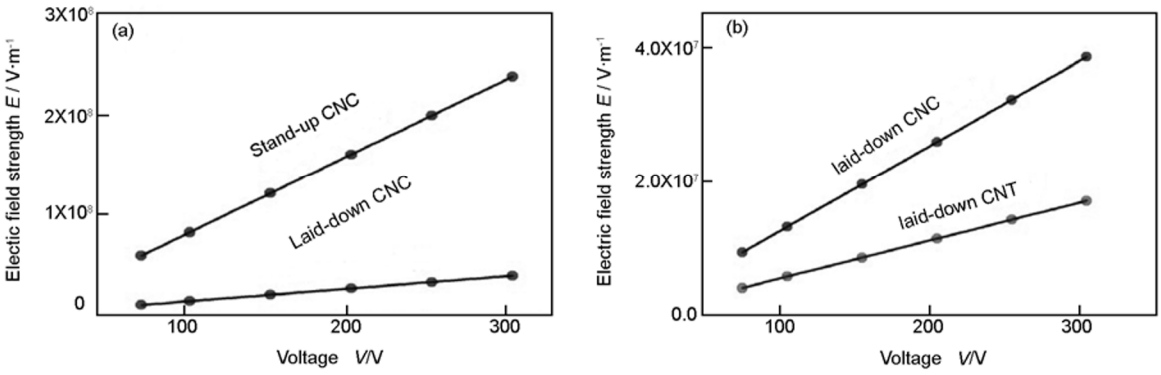

Fig. 6 The relationships between the maximum electric field strength for (a) a stand-up/a laid-down CNC and for (b) a laid-down CNC/CNT with the applied voltages ranging from 75 to 305 V.

Moreover, β for the stand-up CNCs, calculated from the *F-N* plot, is 3.37 times larger than that for the laid-down CNCs.

Fig. 5 shows the electric field strength profiles for the slice around the middle of (a) a stand-up CNC, (b) a laid-down CNC and (c) a laid-down CNT under the anode voltage of 105 V. It is calculated from Fig. 5a and Fig. 5b that the maximum electric field strength on the laid-down CNC (1.33×10^7 V/m) is 6.14 times smaller than that on the stand-up CNC (8.18×10^7 V/m) and is 2.25 times larger than that on the laid-down CNT (5.91×10^6 V/m), which is shown in Fig. 5c.

Fig. 6 shows the relationships between the maximum electric field on (a) a stand-up/laid down CNC and (b) a laid-down CNC/CNT with the applied voltages ranging from 75 to 305 V. Obviously, the maximum electric field on the stand-up CNC, the laid-down CNC and the laid-down CNT increase linearly with the increase of the applied voltages. According to the F-N theory, the field emission factor β equals to F_{local} / F_{appl} [22], where the F_{local} is the field strength concentrated at the field emitter and the F_{appl} is the applied electric field. Therefore, In the Fig. 6a, β for the stand-up and laid-down CNC are constants and their values are 39 and 6.33, respectively. The ratio of β for the both CNCs is 6.14 times, which is larger than the actual measured value of 3.37 times. This is because that the stand-up end of a CNC cannot completely vertical to the substrate due to the elastic force interaction between the stand-up part and the laid-down part. Therefore, the calculated β for the vertically aligned CNC is larger than that for the CNC tilted to the substrate.

In the Fig. 6b, β for the laid-down CNT is also a constant of merely 2.8, which is 2.25 times smaller than that for the laid-down CNC. This is because that the helical morphology of CNC can reduce the screen-effect from the surrounding substrate, so the β for the laid-down CNC is larger than that for the laid-down CNT. Therefore, larger electric field strength is concentrated on the CNCs which are uniformly dispersed on the substrate, resulting in the lower turn-on voltage of the field emission. All these results indicate that the CNC emitter is very fascinating, and suitable for wide applications.

4 Conclusions

CNCs were successfully synthesized by a thermal CVD on the Sn-coated ordinary SS substrate. Calcination temperature plays an important role in the growth of CNCs, and it is believed that the enough fusion of Sn with Fe (Ni) in SS is realized under the calcination temperature at 900 °C. The measurement of field emission from the CNCs dispersed on an n-type Si substrate shows that the turn-on electric field is 1.6 *V*/μm. The corresponding *F-N* plot consists of two straight lines, which attributes to the fact that one ends of some CNCs stand up due to the Coulomb force when the applied voltage is large enough. This result is explained by the calculation for distributions of the electric fields on a stand-up CNC and a laid-down CNC. The distributions of electric fields on a laid-down CNC and a laid-down CNT show that the field enhancement factor β for the laid-down CNC is 2.25 times larger than that for the laid-down CNT. This is because that the helical morphology of CNC can reduce the screen-effect produced by the surrounding substrate.

Acknowledgments

This work was supported by the National Natural Science Foundation of China (51072027, 61137005).

References

[1] Chen X Q, Zhang S L, Dikin D A, et al. Mechanics of a carbon nanocoil[J]. Nano Letters, 2003, 3(9): 1299-1304.

[2] Hayashida T, Pan L J, Nakayama Y. Mechanical and electrical properties of carbon tubule nanocoils[J]. Physical B, 2002, 323: 352-353.

[3] Chang N K, Chang S H. High-yield synthesis of carbon nanocoils on stainless steel. Carbon, 2008, 46(7): 1106-1109.

[4] Ridriguez N M. A review of catalytically grown carbon nanofibers[J]. Journal of Materials Research, 1993, 8(12): 3233-3250.

[5] Pan L J, Zhang M, Nakayama Y. Growth mechanism of carbon nanocoils[J]. Journal of Applied Physics, 2002, 91(12):

10058-10061.

[6] Li D W, Pan L J. Growth of carbon nanocoils using Fe-Sn-O catalyst film prepared by a spin-coating method[J]. Journal of Materials Research, 2011, 26(16): 2024-2032.

[7] Li D W, Pan L J, Wu Y K, et al. The effect of changes in synthesis temperature and acetylene supply on the morphology of carbon nanocoils[J]. 2012, Carbon, 50: 2571-2580.

[8] Saito Y, Uemur S, Hamaguchi K. Cathode ray tube lighting elements with carbon nanotube field emitters. Japanese Journal of Applied Physics[J], 1998, 37(3B): 346-348.

[9] Uemura S, Yotani J, Nagasako T, et al. Large-area FEDs with carbon-nanotube field emitter[J]. Journal of the Society for Information Display, 2003, 11(1): 145-153.

[10] Lee N S, Chung D S, Kang J H, et al. Carbon nanotube-based field-emission displays for large-area and full-color applications[J]. Japanese Journal of Applied Physics, 2000, 39(12B): 7154-7158.

[11] Rupensinghe N L, Chhowalla M, Teo K B K, et al. Field emission vacuum power switch using vertically aligned carbon nanotubes[J]. Journal of Vacuum Science & Technology B, 2003, 21(1): 338-343.

[12] Nilsson L, Groening O, Emmenegger C, et al. Scanning field emission from patterned carbon nanotube films[J]. Applied Physics Letters, 2000, 76(15): 2071-2073.

[13] Gröning O, Küttel O M, Emmenegger Ch, et al. Field emission properties of carbon nanotubes[J]. Journal of Vacuum Science & Technology B, 2000, 18(2): 665-679.

[14] Ding H, Feng T, Chen Y W, et. al. Field emission properties of carbon nanotubes in a stretchable polydimethylsiloxane matrix[J]. Applied Surface Science, 2012, 258: 5191-5194.

[15] Konishi Y, Hokushin S, Tanaka H, et al. Comparison of field emissions from side wall and tip of an individual carbon nanotube[J]. Japanese Journal of Applied Physics, 2005, 44(4A): 1648-1651.

[16] Pan L J, Hayashida T, Zhang M, et al. Field emission properties of carbon tubule nanocoils[J]. Japanese Journal of Applied Physics, 2001, 40(3B): 235-237.

[17] Hokushin S, PAN L J, Konishi Y, et al. Field emission properties and structural changes of a stand-alone carbon nanocoil[J]. Japanese Journal of Applied Physics, 2007, 46(23): L565-L567.

[18] Pan L J, Konishi Y, Tanaka H, et al. Effect of morphology on field emission properties of carbon nanocoils and carbon nanotubes[J]. Japanese Journal of Applied Physics, 2005, 44(4A): 1652-1654.

[19] Sung W Y, Kim W J, Yeon S C, et al. Field emission characteristics of carbon nanocoils grown on copper micro-tips[D]. Vacuum Nanoelectronics Conference, 2006, 101-102.

[20] Zhao Q, Pan L J, Ma H, et al. Structure changes of an individual carbon nanocoil and its field-emission enhancement by laser treatment. Diamond & Related Materials, 2012, (22): 33-36.

[21] Gomer R., Field emission and field ionization[M], AIP, New York, 1992.

[22] Seong C L, Hee J J, Keun S K, et al. Extracting independently the work function and field enhancement factor from thermal-field emission of multi-walled carbon nanotube tips. Carbon, 2005, (43): 2801-2807.